Ceramics-Silikáty 67 (3), 296-305 (2023)
www.ceramics-silikaty.cz doi: 10.13168/cs.2023.0030

PROPERTIES AND ENVIRONMENT IMPACT OF CEMENTITIOUS MATERIALS PREPARED WITH FLUORGYPSUM AND STEEL SLAG

QINGHUI YANG*, YUANTAO WANG*, SHUFENG LIU*, XIN GAO**, YUANYUAN HUANG*, HENGFU ZHANG*, #DELU ZOU*, HAORAN ZHAI*

*Shandong Hi-Speed Urban and Rural Development Group CO., LTD, 250014, Jinan, China
**University of Jinan, School of Architecture and Construction, 250022, Jinan, China

#E-mail: sdgszdl@163.com

Submitted April 29, 2023; accepted July 28, 2023

Keywords: Solid electrolyte, Perovskite, Dope, Conductivity

The industrial by-products of fluorgypsum (FG) and steel slag (SS) were recycled for the preparation of gypsum-based cementitious materials (GBCMs). Na_2SO_4 and $KAl(SO_4)_2$ were applied to activate the hydration of FG and SS, respectively. The properties of the GBCM were investigated. The residual H_2SO_4 and soluble F in the FG poses a great threat to the environment. Hence, the environmental impacts of the GBCM were also studied. The results demonstrate that, with an increase in the SS content of the GBCM, the water requirement for normal consistency increases, the setting times are obviously prolonged, while the mechanical strength and the linear expansion rate are lower. Due to the hydration of SS and the formation of ettringite at a late hydration age, both the compressive strength and flexural strength for FG : SS = 9 : 1 and FG : SS = 8 : 2 are close to that of FG : SS = 10 : 0 at 90 d. The water resistance of the GBCM paste is also improved by adding SS into the FG. Hence, considering the mechanical strength and water resistance, the SS content of the GBCM should not exceed 20 %. The H_2SO_4 in the GBCM can be neutralised by SS. Furthermore a novel quick and effective method, through the precipitation of AlF_3, for the immobilisation of soluble F was proposed. Therefore, FG and SS can be recycled for the production of GBCM without bringing about an adverse environmental impact.

INTRODUCTION

Fluorgypsum (FG) is a by-product of manufacturing hydrofluoric acid resulting from sulfuric acid and fluorite reactions. [1-2]. It mainly consists of II-anhydrite [1, 3-4]. Moreover, it also contains a slight amount of H_2SO_4, soluble F and CaF_2. For 1 tonne of hydrofluoric acid, ~4 tonnes of FG are produced [5-6]. In China, more than 1×10^6 tonnes of FG are discharged annually. However, merely 25 % of this is recycled due to the low hydration activity of II-anhydrite and the soluble F as well as the residual H_2SO_4 [1, 7]. The majority of FG piles up in the open air, which occupies a considerable amount farmland. Furthermore, the residual H_2SO_4 and soluble F could also bring about serious pollution to the air and underground water [8]. Therefore, it is urgent to find methods for the effective recycling of FG.

The acceleration of the hydration of II-anhydrite is a key issue in the recycling of FG for the production of cementitious materials, which endows the FG paste with mechanical strength. At present, sulfates and chlorine salts have been utilised to activate the hydration activity of II-anhydrite [8-11]. Compared with the pastes prepared with hemihydrate gypsum, the paste prepared with activated FG shows a relatively lower hydration rate and a lower compressive strength at the early hydration age. However, the long-term compressive strength is somewhat higher [10-12]. Therefore, FG is a suitable alternate for the preparation of gypsum-based materials with a higher long-term compressive strength.

The poor water resistance of gypsum-based cementitious material is the second factor limiting FG recycling. To improve the water resistance of the gypsum paste prepared with FG, cementitious materials, such as Portland cement (PC), fly ash (FA), granulated blast furnace slag (GBFS), silica fume (SF) and metakaolin (MK), are frequently used. The gypsum-based cementitious materials of FG–FA–PC clinker-slag-lime [13], FG–GBFS–MK [14], FG–PC–GBFS [15] and FG–PC–FA [3, 16-18] have been prepared. However, adding PC, lime, and MK increases the cost and consumes less solid waste. Therefore, to lower the cost and recycle more in-dustrial waste, industrial waste with hydraulic activity must be added to the FG to prepare gypsum-based cementitious materials with good water resistance.

Steel slag (SS) is a by-product generated in steelmaking [19]. Diverse mineral phases have been reported for SS due to the variation in the chemical compositions. The mineral phases include olivine, merwinite (C_3MS_2), tricalcium silicate (C_3S), dicalcium silicate (β-C_2S and

γ-C_2S), tetracalcium aluminoferrite (C_4AF), calcium ferrite (C_2F), RO phase (CaO−FeO−MnO−MgO solid solution), lime, periclase, fluorite (CaF_2) and an amorphous phase [19-20]. Although C_3S, β-C_2S, γ-C_2S and C_4AF are considered to have high hydration activity in Portland cement, the minerals in the SS are considered as slightly active due to the high calcining temperature during steelmaking. However, the hydration activity of SS could be activated by chemicals. A previous study investigated NaOH, K_2SO_4, Na_2SO_4, $KAl(SO_4)_2$, $CaCl_2$, $AlCl_3$ and $NaAlO_2$ on the hydration activity of SS, which caused the SS to possess good long-term cementitious properties [21-22]. The results demonstrate that $KAl(SO_4)_2$ is the best activator for SS [22]. Therefore, when a certain amount of SS is added into FG to prepare gypsum-based cementitious materials, the water resistance of the gypsum-based cementitious material may be improved by adding $KAl(SO_4)_2$.

Another factor limiting the recycling of FG is the slight amount of residual H_2SO_4 and the soluble F [1]. Both H_2SO_4 and the soluble F could seep into underground water and can pollute it. Therefore, the pH value of the hydration products and the immobilisation of the soluble F should be considered when FG and SS are used to prepare GBCMs.

In this study, five GBCMs with an FG to SS ratio (by weight) of 10:0, 9:1, 8:2, 7:3 and 6:4 were prepared. Na_2SO_4 and $KAl(SO_4)_2$ were used to activate the hydration activity of FG and SS, respectively. The water requirement for normal consistency and the setting time, strength development and hydration of the GBCM were studied. In addition, the water absorption, softening coefficient and pore structure of the hardened GBCM pastes were tested. Moreover, the neutralisation of the residual H_2SO_4 and the immobilisation of soluble F in GBCM were also investigated.

EXPERIMENTAL

Materials

Fresh FG (Dongyue Group Ltd., Shandong, China) and SS (Shandong Iron and Steel Group Co., Ltd, Shandong, China) were utilised to prepare the GBCM. The SS was outdoor weathered for three months to promote the complete hydration of the free CaO, which was intended to ensure a volume stability GBCM paste. The phase compositions of FG and weathered SS are shown in Figure 1. The FG is mainly composed of anhydrite and calcium fluoride. For the SS, the crystalline phases are mainly composed of calcite, quartz, an RO phase, calcium silicate (C_2S), merwinite and pyroxene. No $Ca(OH)_2$ was detected in the weathered SS, which is due to that $Ca(OH)_2$ can easily be carbonated to form $CaCO_3$. The chemical compositions of the SS and FG, expressed in oxides, are shown in Table 1.

The FG was dried and milled by a disc mill to pass through a 200-mesh sieve with a residue of 10.3 %. The SS was ground by a ball mill to pass through a 200-mesh sieve with residue of 3.5 %. The particle size distribution of the ground SS and FG are presented in Figure 2.

Table 1. Chemical compositions, expressed in oxides, of the FG and SS (wt. %).

Oxide	CaO	SiO_2	Al_2O_3	Fe_2O_3	MgO	SO_3	MnO	K_2O	TiO_2	P_2O_5	Na_2O	F	Others	LOI
FG	38.62	1.99	0.32	0.21	0.48	54.84	–	-0.14	–	–	0.11	1.09	1.36	0.83
SS	37.06	21.49	8.69	6.23	3.04	0.69	0.95	0.67	0.59	0.29	0.25	–	0.32	19.73

The soluble F content of the FG is 0.37 %, the pH value of the FG is 1.12

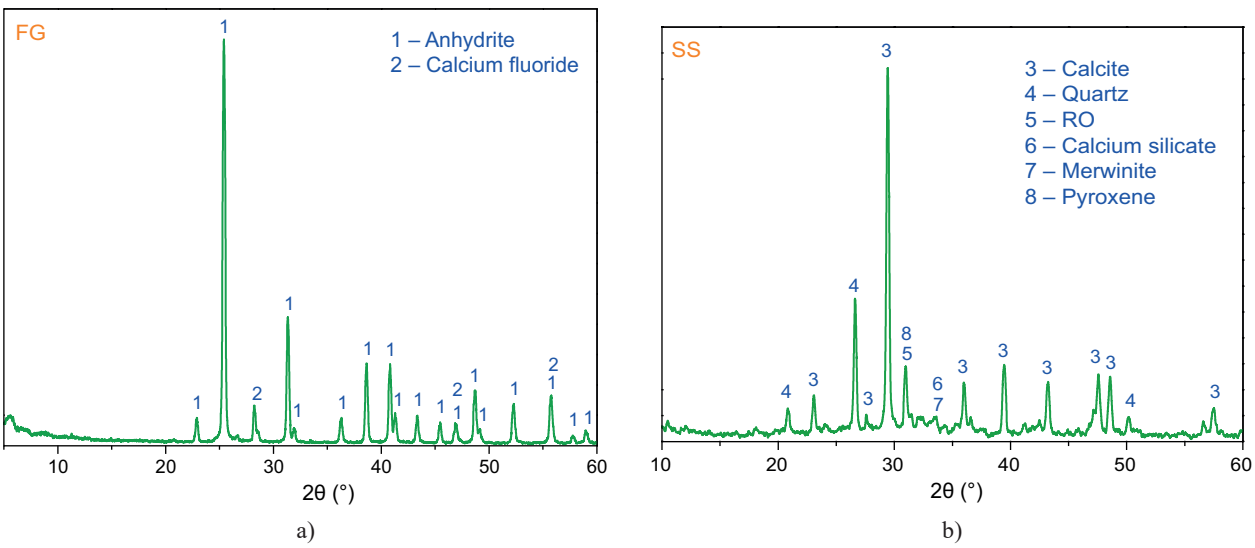

Figure 1. XRD patterns of the FG and weathered SS. (RO is defined as a CaO–FeO–MnO–MgO solid solution).

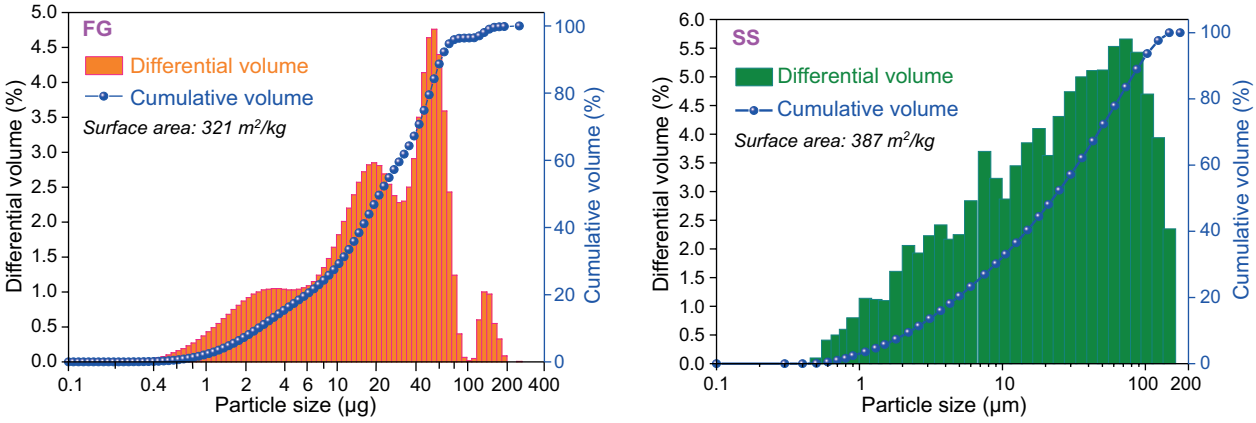

a) b)

Figure 2. Particle size distributions of the FG and SS powders.

The FG and SS were mixed in the following proportions (by weight): 10:0, 9:1, 8:2, 7:3 and 6:4 for the preparation of the GBCM. 2.0 % Na_2SO_4 and 3.5 % $KAl(SO_4)_2$ (industrial grade) were used as the accelerators to promote the hydration of the FG in the GBCM.

Methods

Water requirement for normal consistency and the setting time

The water requirement for normal consistency and the setting time of the GBCM were tested according to the Chinese standard GB/T 9776-2008.

Mechanical strength and linear expansion rate

The samples with dimensions of 40 × 40 × 160 mm and 25 × 25 × 280 mm were applied for testing the mechanical strength and linear expansion rate, respectively. All the samples were prepared with the paste with a water to binder ratio (w/b) of 0.35. The samples in the moulds were firstly cured in a standard chamber at a temperature of (20 ± 1) °C and a humidity of (95 ± 1) % for 24 h. After demoulding, the samples were then cured at (20 ± 1) °C in air. The mechanical strength was measured at the hydration age of 1, 3, 7, 28, and 90 days. Each value of the compressive strength and flexural strength was determined by an average value of six samples and three samples, respectively. The linear expansion rate of the hardened GBCM pates was calculated by Equation 1.

$$\omega = \frac{L_T - L_0}{280} \quad (1)$$

where ω, L_T, L_0 and 280 denote the linear expansion rate, length at the specified age, length of the samples at 24 h and the initial length of the sample, respectively.

Water absorption rate and softening coefficient

The water absorption of the samples was determined by the mass increments for the samples cured in water at (25 ± 1) °C for 2 h and 24 h, respectively. The softening coefficient was characterised by the retention ratio of the compressive strength after 24 h soakage in water.

X-ray fluorescence analysis and particle size distribution

The chemical compositions of the FG and SS were determined by X-ray fluorescence analysis (XRF, S8 TIGER) at 40 kV and 70 mA. The particle size distributions of the FG and SS were measured by a laser particle size analyser (LS13320).

X-ray diffraction analysis

After the termination of the hydration by absolute ethyl alcohol for 12 h, the hydration products of the GBCM pastes were dried at 40 °C in a vacuum oven for 24 h. Then the dried samples were ground to pass through a 76 μm sieve for the X-ray diffraction analysis (XRD, D8 Advance). The measurement was performed with Cu Kα radiation at 40 kV and 40 mA within a 2θ range of (5-65)° with a scan speed of 0.2 s for 0.02°.

Heat release

The heat flow for the hydration of the GBCM was recorded by an eight channel TAM AIR isothermal calorimetric calorimeter using 2 g of GBCM with 1 g of water for 72 h at a constant temperature of 20 °C. The resulting heat flow curves were integrated to obtain the cumulative heat during hydration.

Pore structure analysis

After vacuum drying for 24 h, the pore structure of the hardened GBCM paste was tested by a Mercury intrusion porosimeter (MIP, Quanta, Poremaster-60) within a pressure range of 0-6 × 10^4 psia.

pH value and the leaching behaviour of F for the hydration product

The suspensions with a w/b of 1:1 (by weight) were stirred by a magnetic stirring apparatus for 1 min, 2 min,

5 min, 10 min, 30 min and 60 min. After filtering by a suction filter, the leachates were applied for testing the pH value by an FE28 pH-meter (Mettler Toledo). The F^- concentrations of the leachates were tested by the chemical method, which is provided by the Chinese standard of GB/T 5484-2000. The Al^{3+} concentrations of the leachates were tested by an ICP-AES (Baird, PS-6, USA).

Chemically combined water content

After the termination of the hydration, the hydration products of the GBCM were dried in a vacuum drying oven to remove the free water. Then the samples were calcined at 950 °C for 30 min. Finally, the samples were cooled down to room temperature to a constant weight. The chemically combined water content can be calculated by Equation 2.

$$W = [(m_a - m_b)/m_b - L] \times 100\ \% \qquad (2)$$

where W, m_a, m_b, and L denote the chemically combined water content, weight before calcination, weight after calcination and the weight loss of ignition, respectively.

RESULTS AND DISCUSSIONS

Environmental impact

Generally, the pH value of the FG is within the range of 1.1-2.1 [6], which is attributed to the residual H_2SO_4 and considered highly corrosive. If the residual H_2SO_4 in the FG seeps into the underground water, it can change the pH value of the underground water and pose a great threat to the environmental safety. The pH value of the FG used in this study is 1.12. To avoid any environmental pollution caused by the residual H_2SO_4, it must be neutralised.

The variations of the pH value of the leachates for the hydration products of the GBCM are shown in Figure 3. For FG:SS = 10:0, the pH value of the leachate keeps at a constant value of ~1.10. For the hydration products of the other composite cementing materials, the pH value of the leachate increases dramatically within 0-60 min. Within 10 min, all the pH values for the leachates of the hydration products of the GBCM exceed 7. The weathered SS contains a great deal of $CaCO_3$ (Figure 1), which is considered an alkaline material. Therefore, the residual H_2SO_4 in the GBCM can be easily neutralised.

For human beings, an excessive F intake over a long period of time could lead to fluorosis, which is characterised by dental mottling and skeletal manifestations, such as crippling deformities, osteoporosis and osteosclerosis [31]. For plants, the excessive F in the water could also inhibit the seed germination. Moreover, F could destroy the enzymes in plants, which thereby adversely affects the plant growth [32]. Therefore, the immobilisation of the soluble F is a precondition for the recycling of FG for the production of GBCMs.

The variations in the Al^{3+} and F^- concentrations of the leachates for the hydration products of the GBCM are shown in Figure 4. When prolonging the hydration time, the F^- concentrations in the leachates of the

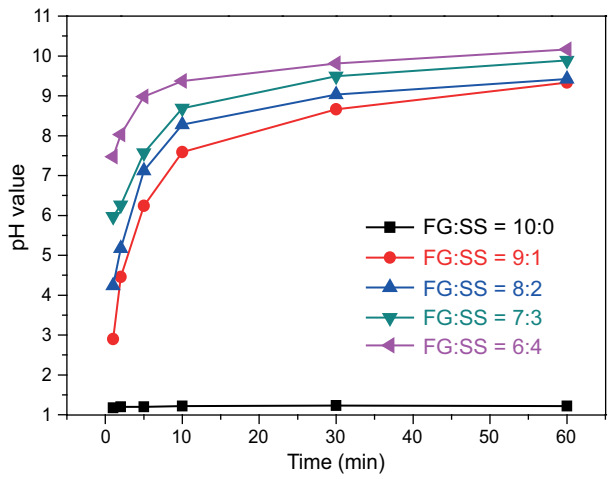

Figure 3. Variations in the pH value of the leachates for the hydration products of the GBCM paste.

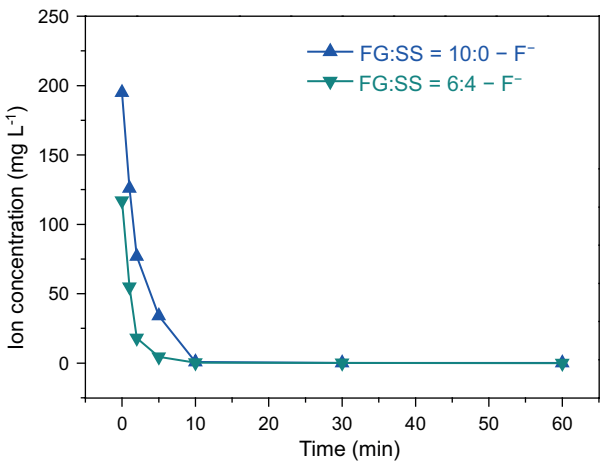

a)

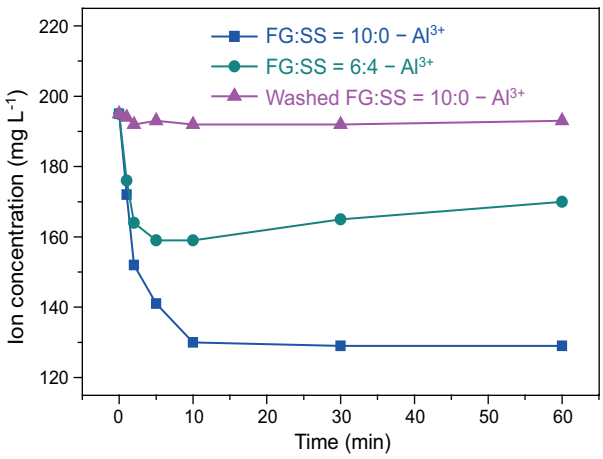

b)

Figure 4. Variation in the Al^{3+} and F^- concentrations of the leachates of the GBCM paste.

FG:SS = 10:0 paste and FG FG:SS = 10:0:SS = 6:4 paste decrease sharply. At 10 min, almost all the F^- is well immobilised. Meanwhile, the Al^{3+} concentrations of the leachates of the FG:SS = 10:0 paste and FG:SS = 6:4 paste decrease sharply within 0-10 min. In the following hydration period, the Al^{3+} concentrations of the leachates keep at a constant value. For the washed FG, all the soluble F has been removed. The Al^{3+} concentration keeps at a constant value. Therefore, it is concluded that the following reaction (Equation 3) takes place and the water insoluble AlF_3 forms.

$$Al^{3+} + 3F^- = AlF_3\downarrow \quad (3)$$

At 10 min, the F^- concentrations of the leachates of the FG:SS = 10:0 paste and FG:SS = 6:4 paste are 0.82 $mg \cdot L^{-1}$ and 0.34 $mg \cdot L^{-1}$, respectively. It is far below the safe level of 1 $mg \cdot L^{-1}$ which is required in the Chinese standard for drinking water [33]. Therefore, it is concluded that FG could be utilised for the production of GBCM without bringing about F pollution.

Properties

Water requirement for normal consistency and setting time

The water requirement for normal consistency and the setting time of the GBCM are shown in Table 2. With the increase in the SS content of the GBCM, the water requirement for normal consistency increases. It is due to the fact that the surface area of the SS is relatively higher than the FG (Figure 1), which increases the contact area between the GBCM and the water and makes it absorb more water.

The setting time of the cementitious materials is defined as the initial solidification and subsequent hardening [23], which is closely related to the workability and early hydration of the minerals. For FG:SS = 10:0, the initial setting time and final setting time are 103 min and 185 min, respectively, which is much longer than the setting time of hemihydrate gypsum [24] due to the fact that the hydration activity of the activated II-anhydrite is lower than hemihydrate gypsum. [24]. For the GBCM paste, the initial solidification and subsequent hardening is caused by the hydration of II-anhydrite to form gypsum. With the increase in the SS content of the GBCM, the FG is diluted and less gypsum forms at the early age. Therefore, both the initial setting time and final setting time are obviously prolonged.

Table 2. Water requirement for the normal consistency and setting time of the GBCM.

FG:SS	Water requirement for normal consistency (%)	Setting time (min)	
		Initial	Final
10:0	34.4	103	185
9:1	34.8	145	226
8:2	35.0	168	258
7:3	35.2	183	277
6:4	35.3	206	295

Strength development

Figure 5 shows the compressive strength and flexural strength development of the GBCM paste. The compressive and flexural strength increase remarkably within the hydration age of 28 d. After 28 d, for FG:SS = = 10:0, the compressive strength and flexural strength keep at a constant value, while the compressive strength and flexural strength for FG:SS = 9:1, FG:SS = 8:2, FG:SS = 7:3 and FG:SS = 6:4 increase. So it is that the hydration of anhydrite dominates the early age strength development to form gypsum. At the late hydration age, $KAl(SO_4)_2$ activates the hydration activity of the SS [22], promoting strength development at the late hydration age.

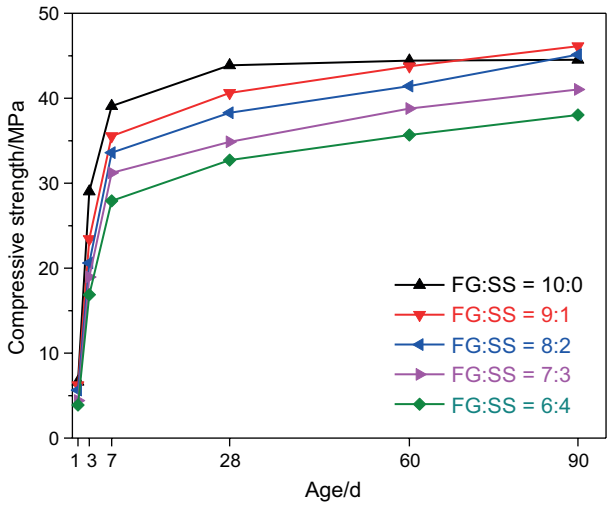

a)

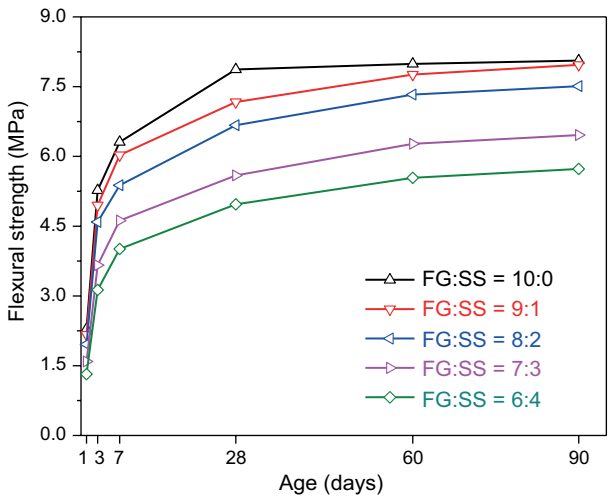

b)

Figure 5. Compressive and flexural strength development of the GBCM paste.

At the hydration age of 90 days, both the compressive strength and flexural strength of FG:SS = 9:1 and FG:SS = 8:2 are close to that of FG:SS = 10:0, while the compressive strength and flexural strength of FG:SS = = 7:3 and FG:SS = 6:4 are much lower than that of FG:SS = 10:0. Therefore, from the perspective of the mechanical strength, the SS content of the GBCM should not exceed 20 %.

Water absorption and softening coefficient

Poor water resistance is the main drawback of gypsum-based cementitious materials [13] and the water resistance is closely tied with the service life of gypsum-based cementitious materials. For gypsum-based cementitious materials with poor water resistance, they are easy to deform and corrupt [25]. Therefore, it is of great importance to improve the water resistance. Usually, a softening coefficient is used to characterise the water resistance of gypsum-based cementitious materials [26].

Figure 6 shows the water absorption and softening coefficient of the hardened GBCM pastes at 90 days. With the increase in the SS content in the GBCM, the water absorption of the hardened GBCM paste decreased from 7.0 % to 5.0 %, the softening coefficient increased from 0.38 to 0.64. This indicates that $KAl(SO_4)_2$ could activate the hydration activity of the SS, which improves the water resistance of the GBCM.

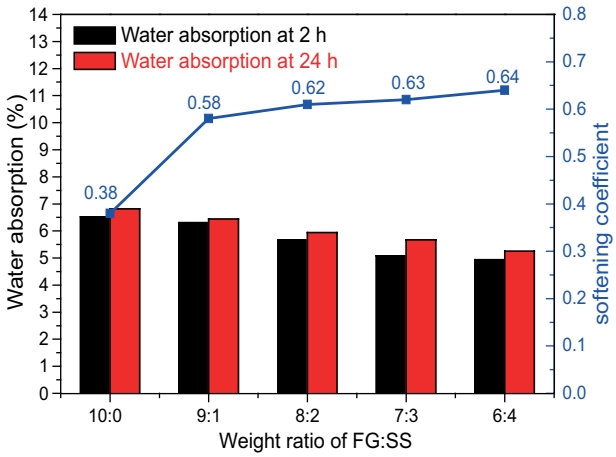

Figure 6. Water absorption and softening coefficient of the GBCM pastes at the hydration age of 90 days.

When the SS contents of the GBCM are 10 % and 20 %, the softening coefficients increase from 0.38 to 0.56 and 0.62, respectively. For the GBCM containing 30 % and 40 % SS, there is merely a slight increase of the softening coefficients. Therefore, taking the water resistance and mechanical strength into consideration, the SS content of the GBCM should not exceed 20 %.

Dimensional stability

Figure 7 presents the dimensional changes to the GBCM. The hardened GBCM pastes present a linear expansion. A previous investigation found the same law in the composite cementitious materials of FG–PC–GBFS [27], FG–GBFS-SF [28] and FG–PC–FA [17] with sulfate as the activators of II-anhydrite. With the increase in the SS content, the linear expansion rate of the GBCM paste presents a downward trend. Within 28 days, the linear expansion rate increases sharply, which is mainly caused by the hydration of anhydrite to form gypsum. After 28 days, the expansion rate of the GBCM paste keeps at a constant value.

Throughout the hydration period, no cracks were observed on the paste. It is attributed to that, after three months of weathering, all the free CaO in the SS has been hydrated and carbonated to form $CaCO_3$, which avoids the volume expansion caused by the hydration of the free CaO [29].

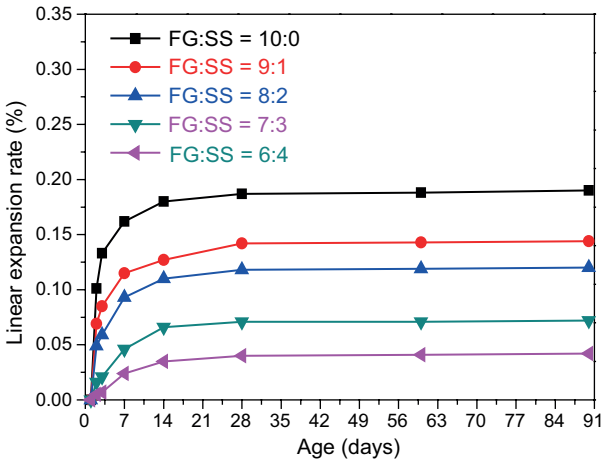

Figure 7. Linear expansion rate for the hardened GBCM paste.

Hydration

To investigate the hydration of GBCM, the heat flow and cumulative heat were tested. Figure 8 shows the hydration heat of GBCM with a w/b of 0.50. The heat flow curve is characterised by one exothermal peak. The obvious endothermic peak observed within 0-0.15 h is caused by the rapid dissolution of Na_2SO_4, $Al_2(SO_4)_3$ and $KAl(SO_4)_2 \cdot 12H_2O$. The exothermal peak within the hydration period of 0.15-72 h is mainly caused by the hydration of FG. With the increase in the SS content in the GBCM, the FG in the GBCM is diluted and less anhydrite hydrates, which thereby results in an obviously decreasing trend of the heat flow. At 72 h, the cumulative hydration heat for FG:SS = 10:0, FG:SS = 8:2 and FG:SS = 6:4 are 91.27 $J \cdot g^{-1}$, 75.02 $J \cdot g^{-1}$ and 47.33 $J \cdot g^{-1}$, respectively. The results are in accordance with the compressive strength and flexural strength at 3 days.

To investigate the variation in the phase composition of the hydration product, the hydration products of the GBCM of FG:SS = 8:2 at the hydration age of 1, 3, 7, 28, and 90 days were used for the XRD analysis

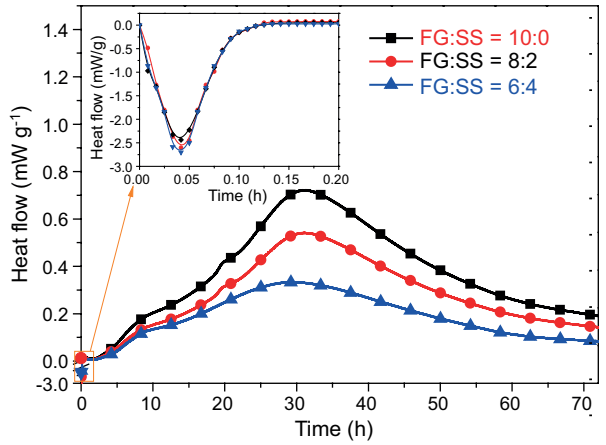

a)

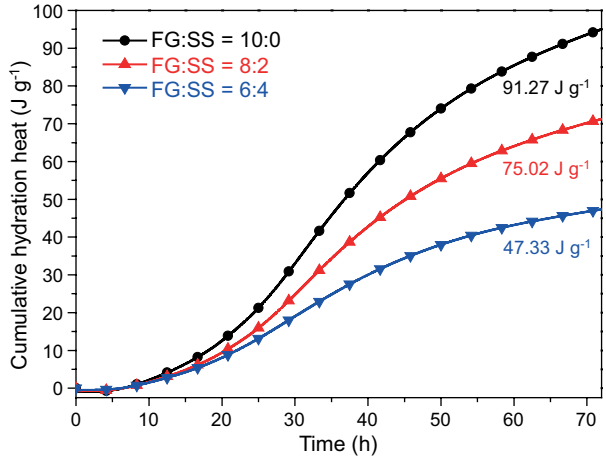

b)

Figure 8. Hydration heat of the GBCM with a water to binder ratio of 0.50.

and the XRD patterns are shown in Figure 9. From 1 to 7 days, the diffraction peak intensity of anhydrite decreases sharply and the diffraction peak intensity of gypsum increases dramatically. At the hydration age of 28 days, the diffraction peak of anhydrite vanishes, which demonstrates that all the FG has hydrated. At the same time, the diffraction peak of AFt is observed, demonstrating that the Ca and Al in the SS react with the gypsum to form AFt in the later hydration period. In the early stage of hydration, the rapid hydration of f-CaO generates $Ca(OH)_2$, which provides polar OH^- ions for the hydration reaction of SS (Eqation 2), which breaks the Si–O–Si, Si–O–Al and Al–O–Al bonds on the surface of SS, prompting it to disperse and dissolve. The Ca^{2+} and $[AlO_2]^-$ dissolved by the SS react rapidly with the $[SO_4]^{2-}$ and Ca^{2+} provided by gypsum to form ettringite (Ettringite or AFt), and the $[SiO_4]^{4+}$ and Ca^{2+} dissolved by the SS with H_2O to form calcium silicate hydrate (C–S–H). Therefore, the mechanical strength of FG:SS = 9:1, FG:SS = 8:2, FG:SS = 7:3, FG:SS = 6:6 increases and the water resistance is improved at the later hydration period.

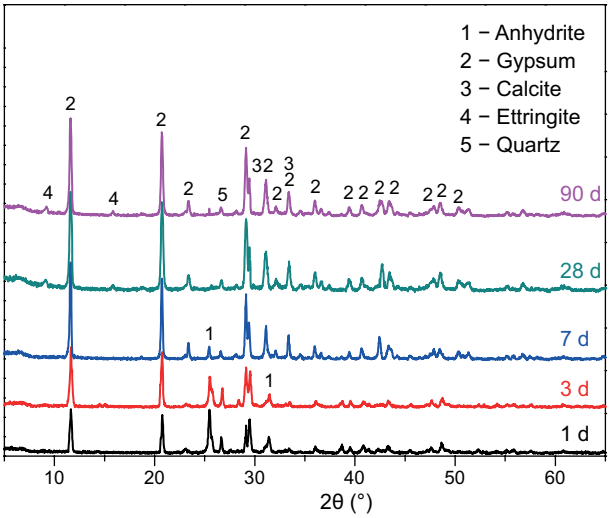

Figure 9. XRD patterns of the hydration products of the GBCM of FG:SS = 8:2 at the hydration age of 1, 3, 7, 28, and 90 days.

To investigate the hydration of SS activated by $KAl(SO_4)_2$ at the late hydration age, the chemically combined water content of the hydration product of the GBCM at 1, 3, 7, 28, and 90 days were tested and the results are shown in Figure 10. For FG: SS=10:0, within the hydration age of 28 days, the chemical combined water content increases when prolonging the hydration age. After 28 days, the chemically combined water content keeps at a constant value. It demonstrates that the hydration of anhydrite mainly occurs within the hydration age of 28 days. For FG:SS = 9:1, FG:SS = 8:2, FG:SS = = 7:3 and FG:SS = 6:4, the chemically combined water content increases within the hydration age of 28-90 d. It is concluded that $KAl(SO_4)_2$ could promote the hydration of SS after 28 days. Therefore, the compressive strength, flexural strength and the softening coefficient present an increasing trend.

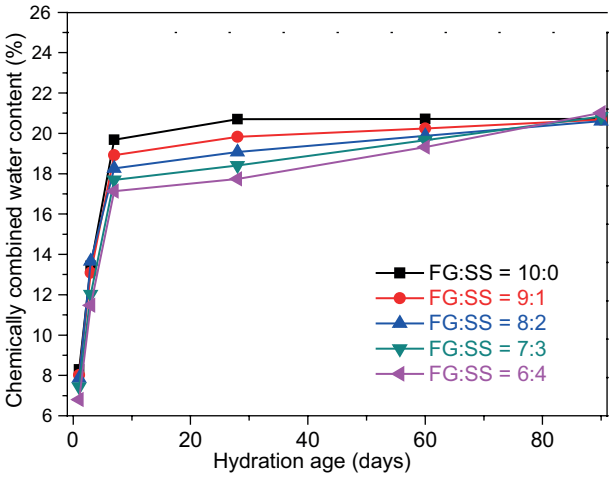

Figure 10. Chemically combined water content of the hydration product of GBCM at 1, 3, 7, 28, and 90 days.90 days.

Pore structure

MIP was applied to reveal the relationship between the pore structure and water absorption of the hardened GBCM pastes. The pore structures of the hardened GBCM pastes of FG:SS = 10:0, FG:SS = 8:2 and FG:SS = 6:4 at the hydration age of 90 days are shown in Figure 11. Based on the pore size, the pores of the cementitious materials can be classified into the four types [30]: gel pore (diameter < 0.01 μm), transition pore (diameter, 0.01-0.1 μm), capillary pore (diameter, 0.1-1 μm) and macroscopic pore (diameter > 1 μm). With the increase in the SS content in the GBCM, the capillary pores and macropores decrease, whereas the transition pores increase. It is mainly attributed to the following reasons: i) the hydration products of SS and the ettringite could fill the pores. ii) compared with FG, the particle size of SS is smaller and the fine SS could fill the macropores.

At the hydration age of 90 days, the porosity of the hardened GBCM of FG:SS = 10:0, FG:SS = 8:2 and FG:SS = 6:4 are 24.01 %, 25.90 % and 27.51 %, respectively. Although the porosity increases, the amount of capillary pores and macropores decrease. The water could enter the capillary pores and macropores, whereas it is hard to enter the transition pores. Therefore, compared with FG:SS = 10:0, the water absorption decreases for FG:SS = 9:1, FG:SS = 8:2, FG:SS = 7:3 and FG:SS = 6:4 (Figure 6).

The pore structure development of the hardened GBCM pastes of FG:SS = 8:2 at the hydration age of 1, 3, 7, 28, and 90 days is shown in Figure 12. When prolonging the hydration age, the pore diameters shift toward a smaller size and the total pore volume decreases gradually. From 1 to 90 days, the porosities of the hardened GBCM pastes lowered from 41.03 % to 24.51 %, contributing to the strength development of the GBCM. Within the hydration age of 28 days, the refinement of the pores is mainly caused by the hydration of FG to form gypsum. After the hydration age of 28 days, almost all the FG has hydrated (Figure 9). Therefore, it is concluded that the refinement of the pore

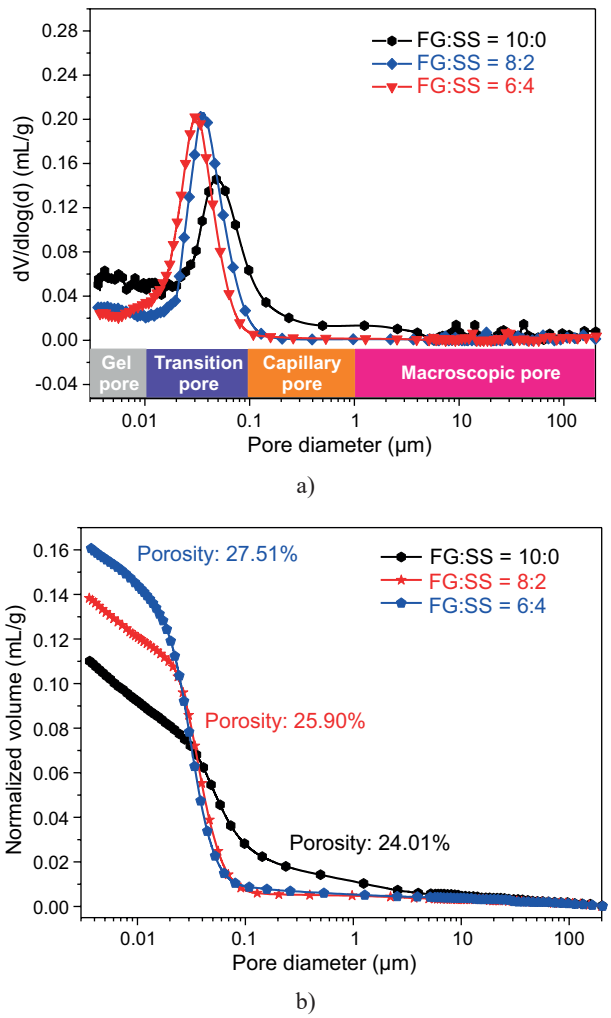

Figure 11. Pore structure of the hardened GBCM pastes of FG:SS = 10:0, FG:SS = 8:2 and FG:SS = 6:4 at the hydration age of 90 days.

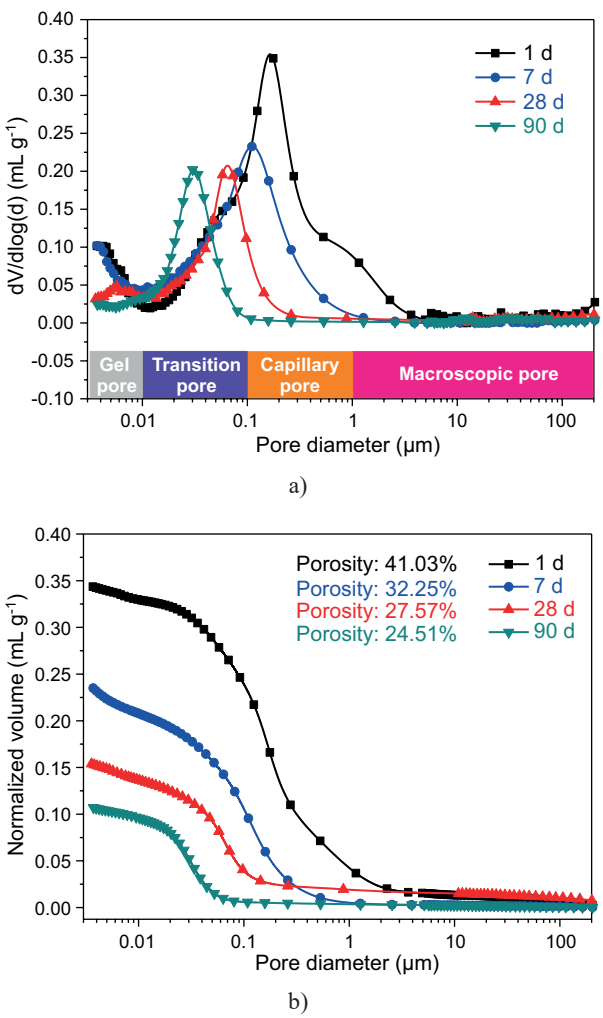

Figure 12. Pore structure development of the hardened GBCM pastes of FG:SS = 8:2 at the hydration age of 1, 3, 7, 28, and 90 days.

structure is mainly caused by the following reasons: i) the ettringite formed after 28 days fills the pores (Figure 9). ii) $KAl(SO_4)_2$ activates the hydration activity of SS at the late hydration age and the hydration products fill the pores.

CONCLUSIONS

In this paper, FG and SS were used to prepare gypsum-based cementitious materials (GBCMs). The properties and environmental impacts of the GBCM were studied. The following conclusions can be drawn from the study:

- With the increase in the SS content of the GBCM, the water requirement for normal consistency increases, the initial and final setting time are obviously prolonged, the linear expansion rate decreases.
- With the increase in the SS content of the GBCM, the mechanical strength decreases. Due to the hydration of SS and the formation of ettringite at the late hydration age, both the compressive strength and flexural strength of FG:SS = 9:1 and FG:SS = 8:2 are close to that of FG:SS = 10:0 at 90 days.
- $KAl(SO_4)_2$ could activate the hydration of SS at the late hydration age. The hydration of SS and the formation of ettringite contribute to the improvement in the water resistance. Taking the mechanical strength and water resistance into consideration, the SS content of GBCM should not exceed 20 %.
- The H_2SO_4 of the GBCM can be neutralised by SS and the soluble F can be immobilised through the precipitation of AlF_3. Therefore, it is concluded that FG and SS can be recycled for the preparation of GBCMs without bringing about any adverse environmental impacts.

REFERENCES

1. Yao Y., Yang D.W., Tong H.X., Zeng J.L., Liu Y. (2011): Modification of waste fluorgypsum and its application as a cement retarder. *Journal of Central South University*, *18*(5), 1402−1407. Doi: 10.1007/s11771−011−0853−9
2. Li R.Y. (2006). Exploration and practice of comprehensive utilization of fluorgypsum residue (in Chinese). *Safety Environ. Eng. 13*, 55−58.
3. Yan P., You Y. (1998): Studies on the binder of fly ash-fluorgypsum-cement. *Cement and Concrete Research*, *28*(1), 135-140. Doi: 10.1016/S0008-8846(97)00247-0
4. Barnes P., Bensted J. (2001). *Structure and Performances of Cements.* New York: Spom Press.
5. Wang J., Yang X., Yu D. (2007): Modification of fluorgypsum as cement retarder. *Journal of Wuhan University of Technology-Mater. Sci. Ed.*, *22*(4), 745-748. Doi: 10.1007/s11595-006- 4745-z
6. Huang X., Zhou M., Hou H., Zhu X., Rong H. (2012): Properties and mechanism of mine tailings solidified and filled with fluorgypsum-based binder material. *Journal of Wuhan University of Technology-Mater. Sci. Ed.*, *27*(3), 465-470. Doi:10.1007/s11595-012-0486-3
7. Yang M., Guo Z.H., Wei X.Y., Xiao X.Y. (2010): Modification and comprehensive utilization of fluorgypsum (in Chinese), Organo-Fluorine Industry, 1, 9−14.
8. Chen C., Habert G., Bouzidi Y., Jullien A. (2010): Environmental impact of cement production: detail of the different processes and cement plant variability evaluation. *Journal of Cleaner Production*, *18*(5), 478-485. Doi: 10.1016/j.jclepro.2009.12.014
9. Sievert T., Wolter A., Singh N. B. (2005): Hydration of anhydrite of gypsum ($CaSO_4$. II) in a ball mill. *Cement and Concrete Research*, *35*(4), 623-630. Doi: 10.1016/j.cemconres.2004.02.010
10. Singh N. B. (2005): The activation effect of K_2SO_4 on the hydration of gypsum anhydrite, $CaSO_4$ (II). *Journal of the American Ceramic Society*, *88*(1), 196-201. Doi: 10.1111/j.1551-2916.2004.00020.x
11. Singh M., Garg M. (2005): Study on anhydrite plaster from waste phosphogypsum for use in polymerised flooring composition. *Construction and Building Materials*, *19*(1), 25-29. Doi: 10.1016/j.conbuildmat.2004.04.038
12. Khalil A. A., Tawfik A., Hegazy A. A., El-Shahat M. F. (2013): Effect of different forms of silica on the physical and mechanical properties of gypsum plaster composites. *Materiales de construcción*, *63*(312), 529-537.
13. Zhou M., Zhang W., Hou H., Huang X., Wang W. (2011): The activation of fluorgypsum with slag activator and the fluorine solidification mechanics. *Journal of Wuhan University of Technology-Mater. Sci. Ed.*, *26*(5), 1023-1026. Doi: 10.1007/s11595-011-0355-5
14. Fraire-Luna P. E., Escalante-Garcia J. I., Gorokhovsky A. (2006): Composite systems fluorgypsum–blastfurnance slag–metakaolin, strength and microstructures. *Cement and Concrete Research*, *36*(6), 1048-1055. Doi: 10.1016/j.cemconres.2006.02.017
15. Garg M., Pundir A. (2014): Investigation of properties of fluorogypsum-slag composite binders–hydration, strength and microstructure. *Cement and Concrete Composites*, *45*, 227-233. Doi: 10.1016/j.cemconcomp.2013.10.010
16. Escalante-Garcia J. I., Rios-Escobar M., Gorokhovsky A., Fuentes A. F. (2008): Fluorgypsum binders with OPC and PFA additions, strength and reactivity as a function of component proportioning and temperature. *Cement and Concrete Composites*, *30*(2), 88-96. Doi: 10.1016/j.cemconcomp.2007.05.015
17. Yan P., Yang W., Qin X., You Y. (1999): Microstructure and properties of the binder of fly ash-fluorogypsum-Portland cement. *Cement and Concrete Research*, *29*(3), 349-354. Doi: 10.1016/S0008-8846(98)00214-2
18. Yan P., Yang W. (2000): The cementitious binder derived with fluorogypsum and low quality of fly ash. *Cement and Concrete Research*, *30*(2), 275-280. Doi: 10.1016/S0008-8846(99)00245-8
19. Shi C. (2004): Steel slag—its production, processing, characteristics, and cementitious properties. *Journal of Materials in Civil Engineering*, *16*(3), 230-236. Doi: 10.1061/(ASCE)0899-1561(2004)16: 3(230)
20. Das B., Prakash S., Reddy P. S. R., Misra V. N. (2007): An overview of utilization of slag and sludge from steel industries. *Resources, Conservation and Recycling*, *50*(1), 40-57. Doi: 10.1016/j.resconrec.2006.05.008

21. Wen J. (2013). *Study on the activation and utilization of steel slag* (Thesis in Chinese), Central South University, Changsha.
22. Zhu J. (2014). *Study on the preparation of steel slag/industrial gypsum composite material* (Thesis in Chinese), University of Jinan, Jinan.
23. Ma B., Ma M., Shen X., Li X., Wu X. (2014): Compatibility between a polycarboxylate superplasticizer and the belite-rich sulfoaluminate cement: Setting time and the hydration properties. *Construction and Building Materials*, *51*, 47-54. Doi: 10.1016/j.conbuildmat.2013.10.028
24. Chen X., Gao J., Liu C., Zhao Y. (2018): Effect of neutralization on the setting and hardening characters of hemihydrate phosphogypsum plaster. *Construction and Building Materials*, *190*, 53-64. Doi: 10.1016/j.conbuildmat.2018.09.095
25. Khalil A. A., Tawfik A., Hegazy A. A. (2018): Plaster composites modified morphology with enhanced compressive strength and water resistance characteristics. *Construction and Building Materials*, *167*, 55-64. Doi: 10.1016/j.conbuildmat.2018.01.165
26. Wu Q., Ma H., Chen Q., Gu B., Li S., Zhu H. (2019): Effect of silane modified styrene-acrylic emulsion on the waterproof properties of flue gas desulfurization gypsum. *Construction and Building Materials*, *197*, 506-512. Doi: 10.1016/j.conbuildmat.2018.11.185
27. Martinez-Aguilar O. A., Castro-Borges P., Escalante-García J. I. (2010): Hydraulic binders of Fluorgypsum–Portland cement and blast furnace slag, stability and mechanical properties. *Construction and Building Materials*, *24*(5), 631-639. Doi: 10.1016/j.conbuildmat.2009.11.006
28. Magallanes-Rivera R. X., Escalante-García J. I. (2014): Hemihydrate or waste anhydrite in composite binders with blast-furnace slag: Hydration products, microstructures and dimensional stability. *Construction and Building Materials*, *71*, 317-326. Doi: 10.1016/j.conbuildmat.2014.08.054
29. Motz H., Geiseler J. (2001): Products of steel slags an opportunity to save natural resources. *Waste Management*, *21*(3), 285-293. Doi: 10.1016/S0956-053X(00)00102-1
30. Yu J., Qian J., Tang J., Ji Z., Fan Y. (2019): Effect of ettringite seed crystals on the properties of calcium sulphoaluminate cement. *Construction and Building Materials*, *207*, 249-257. Doi: 10.1013/j.conbuildmat2019.02.130
31. Fordyce F.M. (2011). *Fluorine: human health risks, Encyclopedia of Environmental Health*, pp. 776–785. Doi: 10.1016/B978-0-444-52272-6.00697-8
32. Zhou H.Q., Chen X.Q., Cheng Q.L. (1996): Effects of fluorine-containing waste gas on the agricultural environment (in Chinese). *Chem. Ind. Environ. Protect. 16*, 98–101.
33. GB 5749-2006. Standards for drinking water (in Chinese).